Nanostructural Organization in Ionic Liquids

José N. A. Canongia Lopes[†] and Agílio A. H. Pádua[‡,*]

Centro de Química Estrutural, Instituto Superior Técnico, Lisboa, Portugal, and Laboratoire de Thermodynamiques des Solutions et des Polymeres, Universite Blaise Pascal Clermont-Ferand, 24, Av. des Landais, Aubiere, 63177 France

Received: October 20, 2005; In Final Form: January 4, 2006

Nanometer-scale structuring in room-temperature ionic liquids is observed using molecular simulation. The ionic liquids studied belong to the 1-alkyl-3-methylimidazolium family with hexafluorophosphate or with bis(trifluoromethanesulfonyl)amide as the anions, $[C_n\text{mim}][PF_6]$ or $[C_n\text{mim}][(CF_3SO_2)_2N]$, respectively. They were represented, for the first time in a simulation study focusing on long-range structures, by an all-atom force field of the AMBER/OPLS_AA family containing parameters developed specifically for these compounds. For ionic liquids with alkyl side chains longer than or equal to C_4, aggregation of the alkyl chains in nonpolar domains is observed. These domains permeate a tridimensional network of ionic channels formed by anions and by the imidazolium rings of the cations. The nanostructures can be visualized in a conspicuous way simply by color coding the two types of domains (in this work, we chose red = polar and green = nonpolar). As the length of the alkyl chain increases, the nonpolar domains become larger and more connected and cause swelling of the ionic network, in a manner analogous to systems exhibiting microphase separation. The consequences of these nanostructural features on the properties of the ionic liquids are analyzed.

Introduction

Room-temperature ionic liquids (RTILs) are low-melting organic salts whose unique properties have been leading to an increasing number of applications as solvents or reaction media. Some of those properties were interpreted as the result of structural features of the liquid phase at the molecular level.[1]

One of the most widely used and studied ionic liquid families is the one based on imidazolium cations, in particular 1-alkyl-3-methylimidazolium hexafluorophosphates $[C_n\text{mim}][PF_6]$. The cations are composed of a polar headgroup, where most of the electrostatic charge is concentrated, and of a nonpolar alkyl side chain, whereas the PF_6^- anion is octahedral, hence almost spherical. The main difference between RTILs and simple molten salts[2,3] is the molecular asymmetry built into (at least one of) the ions, usually the cation, as in the example given. This asymmetry opposes the strong charge ordering due to the ionic interactions that normally would cause the system to crystallize, and thus, a wide liquid range is obtained. Due to the molecular structure of the cations in $[C_n\text{mim}][PF_6]$ ILs, liquid crystalline phases are observed for alkyl side chains longer than dodecyl, but up to C_{12}, the liquid phase is isotropic.[4]

To our knowledge, Compton was the first author to postulate that ionic liquids containing dissolved water "may not be regarded as homogeneous solvents, but have to be considered as nano-structured with polar and nonpolar regions",[5] to explain the large differences in the diffusion of neutral and charged solutes that are observed when comparing dry and wet ionic liquids. These authors did not extend such a hypothesis to pure ionic liquids, but one of them considered the existence of hydrogen-bond networks.[6]

Such hydrogen-bond networks observed in solution[7] are also found in the solid phase. In fact, the structure of some ILs that are solid at room temperature was determined by X-ray diffraction methods[8] and, in the case of $[C_n\text{mim}]^+$ ILs, the structures show that the solid consists of an extended network of cations and anions connected together by hydrogen bonds (through the aromatic hydrogens of the imidazolium ring but also through the hydrogen atoms of the methyl or methylene groups directly attached to the ring), with each cation surrounded by at least three anions and each anion surrounded by at least three cations. Although the number of anions that surround the cation (and vice-versa) can change depending upon the anion size and the imidazolium alkyl substituents, this hydrogen-bonded network of ions is a common feature of imidazolium crystals[6] that is retained in the liquid phase.

Neutron diffraction analysis can yield the complementary liquid structure information. In the case of the dialkylimidazolium systems, a close relationship between the crystal structure and the liquid structure was found, emphasizing once again the importance of the hydrogen-bonding interactions between ions.[9] The existence of hydrogen-bonded clusters both in the solid and liquid phases was also confirmed by IR and Raman spectroscopy,[10−12] NMR,[13] and mass spectrometry.[14,15]

The dual nature of $C_n\text{mim}^+$ ionic liquids, in terms of their ability to interact through electrostatic and dispersive forces, was demonstrated through their use as stationary phases in chromatography.[16] It was found that some IL stationary phases could retain both polar and nonpolar molecules and, surprisingly, that separation and selectivity for the series of normal alkanes was excellent.

Watanabe et al.[17] have studied the dependence of viscosity, diffusion, and ionic conductivity on the alkyl-chain length in $[C_n\text{mim}][(CF_3SO_2)_2N]$ ionic liquids, with $n = 1, 2, 4, 6$, and 8. They observed that viscosity increases and that both the self-diffusion coefficient and the "ionicity", or "degree of ion

* To whom correspondence should be addressed. E-mail: agilio.padua@univ-bpclermont.fr.
† Instituto Superior Técnico.
‡ Université Blaise Pascal/CNRS.

10.1021/jp056006y CCC: $33.50
Published on Web 01/31/2006

dissociation", decrease with increasing chain length. This is a somewhat surprising result, since one would expect at first view that, as the side-chain length increases, the overall contribution of the strong, associating electrostatic (and hydrogen-bond) terms to the interactions diminishes, while the contribution of weaker, nonassociating dispersion forces increases. As a consequence, it could be anticipated that the viscosity would decrease as the size of the nonpolar part of the cations becomes larger. Evidently, this is not the case. The justification put forward by several authors[18,17] is that it is the increase in the van der Waals interactions due to the presence of a long alkyl chain that leads to higher viscosities. But, this argument seems to arise from a simple correlation of what is observed, not having a strong molecular basis. These authors therefore focused on the relative importance of electrostatic and dispersive interactions but still considered the ionic liquids to be structured like a "simple molten salt"[2] (charge-ordering structure) and did not postulate the existence of separate microdomains.

Molecular modeling is a powerful tool to access condensed-phase structure, but most of the simulation studies with ILs carried out so far concentrated on the local scale around a given cation or anion,[19−23] providing results that agree with many of the structural features found in diffraction experiments.[9]

On the basis of computer simulation, the long-range structure of ionic liquids was discussed by Urahata and Ribeiro,[24] who, using a united-atom model of imidazolium ILs, obtained static structure factors showing low wave-vector peaks that are not characteristic of simple molten salts. Those peaks became more evident as the alkyl side-chain increased from C_1 to C_4 and then to C_8, indicating long-range ordering. Wang and Voth[25] very recently reported a computer simulation study, done using a coarse-grained model for the imidazolium ILs, where tail-group (side-chain) aggregation is observed, while the cation head-groups and the anions show homogeneous distributions. Even with such a simplified model, these authors observed tail aggregation for systems corresponding to the range C_4 to C_8 but no aggregation for shorter chains. These authors suggested that "the aggregation of tail groups should clearly exist in most organic ionic liquid systems".[25]

In the present work, we use for the first time atomistic simulation to focus on the nanoscale structuring of $C_n$mim$^+$ salts in the liquid phase, with $n = 2$ up to 12, and study the effect of varying the length of the alkyl side-chain in the cations on the long-range structures.

Results and Discussion

When studying microstructured fluids, the size of the systems and the duration of the simulations are of particular importance: periodic boundary conditions can induce artificial finite-size effects on the length scales of the observed nanostructures,[26] and the slow dynamics of ionic liquids require long simulations. Even facing these exigences, we opted to represent the systems by an all-atom force field,[27,28] which is based on the AMBER/OPLS_AA framework[29,30] but was to a large extent developed specifically for ionic liquids. We estimated that accurate conformational energetics and finely detailed electrostatic charge distributions are relevant when trying to render subtle energetic or configurational features, such as the ones responsible for the nanostructuring.

The molecular dynamics runs were performed using the DL_POLY program[31] on cubic boxes at $T = 300$ K. Simulations were run with different system sizes: 256, 500, and 700 ions. For the heaviest of the ionic liquids, [C_{12}mim][PF_6], the large system contained 19 600 atoms. Equilibrations starting from a low density arrangement of ions took 500 ps. They were followed by trajectories of 500 ps at constant (N, p, T), $p = 0.1$ MPa. Ewald summation was used to account for the long range interactions. We will discuss here almost exclusively the results obtained with the large systems, since those are less prone to artificially induced periodic structures.

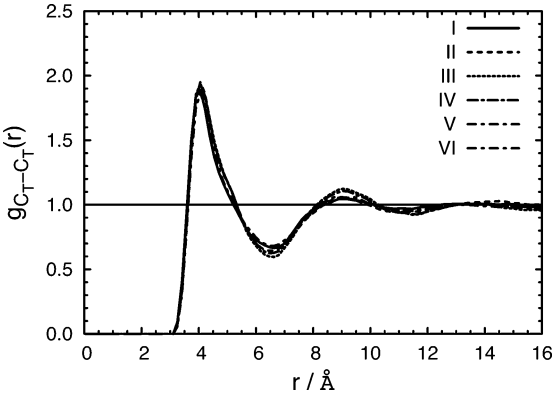

Figure 1. Site−site intermolecular radial distribution function of the terminal carbon of the alkyl side-chain in 1-butyl-3-methylimidazolium hexafluorophosphate, after several independent simulations.

Ionic liquids of the alkylimidazolium family have slow microscopic dynamics[32] with the diffusive regime attained only after trajectories of the order of 1 ns. To ensure that the present results are statistically signifficant, simulations starting from independent equilibrated configurations ware performed and their results were compared. First, a simulation box was equilibrated as indicated above and a production run was executed. Starting with the last configuration of the production run, the system was then ran for 200 ps at 400 K without electrostatic interactions, under a pressure of 30 MPa to avoid vaporization. In this manner, the main force contributing to the spacial organization of the ionic liquid was removed and the mobility of the now uncharged "ions" was greatly augmented. (In fact, this uncharged system seems to evolve toward a demixing of "cations" and "anions".) Then, the electrostatic terms were reactivated and the system was again equilibrated at 300 K and 0.1 MPa for 200 ps. Finally, a new production run of 200 ps was executed. The procedure consisting of a high-temperature anealing of the uncharged system followed by a reequilibration with the full force field was repeated several times. The radial distribution functions obtained from the different cycles are in close agreement, as demonstrated by the example in Figure 1.

The first indication that clustering of the nonpolar side-chains in pure ionic liquids was occurring arose from an analysis of the intermolecular end-carbon to end-carbon site−site radial distribution function (RDF). As shown in Figures 1 and 2, a marked first peak is present for C_4, C_6, and C_8, indicating clustering of the alkyl tails. Such a marked peak is absent in C_2, meaning that in this IL the nonpolar chains are too small and are found to be "diluted" in a medium where strong electrostatic interactions prevail. Such a medium is formed by the anions and by the imidazolium rings of the cations, where the positive charge is concentrated.[27]

To identify more precisely which parts of the ions can be considered to be forming the "charged" and the "nonpolar" regions, the partial charge distributions generated for the molecular force field[27,28] were inspected. Atoms that we assign to the charged regions are, in the imidazolium cations, those of the imidazolium ring, plus atoms bonded to these, and also hydrogens bonded to the first carbons of the alkyl chains (those

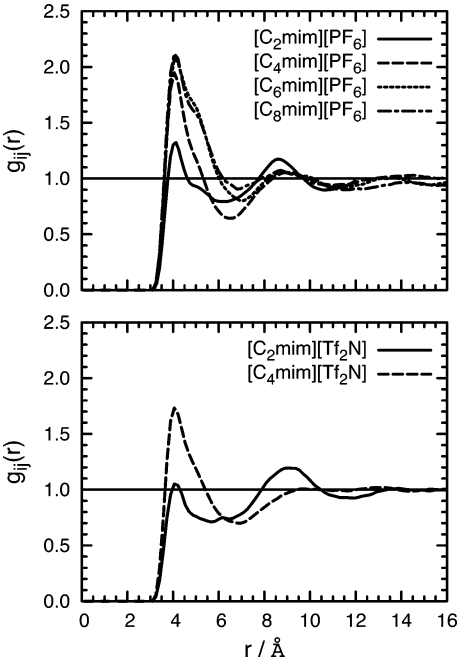

Figure 2. Site−site intermolecular radial distribution functions of the terminal carbon of the alkyl side-chain in several ionic liquids composed of 1-alkyl-3-methylimidazolium cations and PF_6 or $(CF_3SO_2)_2N^-$ anions.

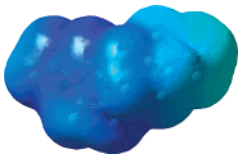

Figure 3. Mapping of the electrostatic potential onto an isoelectronic density surface obtained ab initio at the MP2 level (darker blue shades represent more positive regions) in the C_4mim^+ cation. Details of the calculations can be found in the literature.[27]

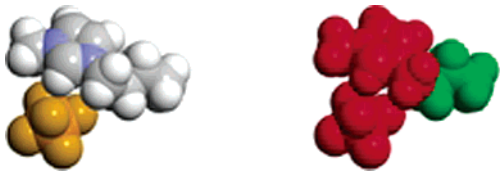

Figure 4. Coloring code used to distinguish the "polar" from the "nonpolar" regions of the ions: (left) Corey, Pauling, Koltun (CPK) coloring; (right) red/green coloring. The example given is $[C_4mim][PF_6]$.

connected to the imidazolium nitrogens); atoms that we identify as forming the nonpolar region of the ion are those from C_2 in the alkyl chains onward. The rationale for such a division is illustrated in the electrostatic surface potential plot in Figure 3. In anions such as BF_4, PF_6, $CF_3SO_3^-$, and $(CF_3SO_2)_2N^-$, all atoms belong to the charged set.

Visualization of the charged and nonpolar domains that eventually form in the liquid phase can be achieved in a very effective way by applying a coloring code: red was chosen for the atoms of the charged or "polar" regions, and green, for those of the nonpolar ones, as in Figure 4. Examples of simulation boxes containing ionic liquids are shown in Figure 5.

The results of the present study agree with those of Wang and Voth[25] concerning the broad picture, but our use of an explicit-atom model provided additional detail. The distribution of the charged domains is not homogeneous, but instead, it has the form of a continuous tridimensional network of ionic channels, coexisting with the nonpolar domains which form, in some cases, dispersed microphases (in C_2) or, in others, continuous ones (in C_{12}).

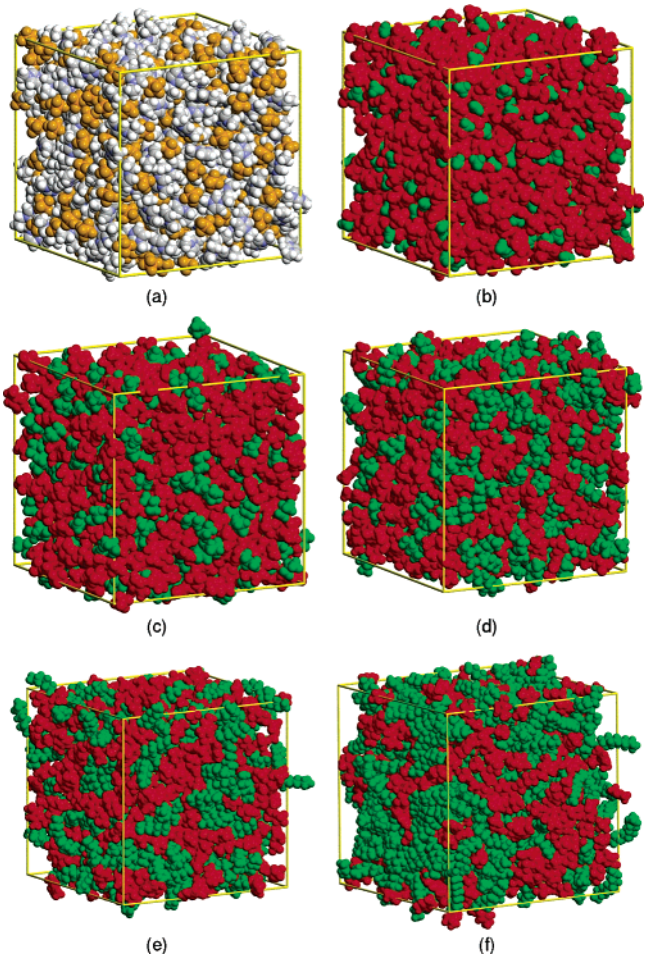

Figure 5. Snapshots of simulation boxes containing 700 ions of $[C_nmim][PF_6]$. The application of a coloring code enables clear identification of the charged and nonpolar domains that form in ionic liquids. The lengths of the box sides are given: (a) $[C_2mim][PF_6]$ CPK coloring; (b) $[C_2mim][PF_6]$ same configuration as in a with red/green (charged/nonpolar) coloring; (c) $[C_4mim][PF_6]$ $l = 49.8$ Å; (d) $[C_6mim][PF_6]$ $l = 52.8$ Å; (e) $[C_8mim][PF_6]$ $l = 54.8$ Å; (f) $[C_{12}mim][PF_6]$ $l = 59.1$ Å.

The simulation snapshots of Figure 5, especially those rendered under the red/green polar/nonpolar convention, provide a powerful visual insight into the nature and evolution of the observed structures as the length of the nonpolar chain is increased. However, a more complete analysis can be performed if the radial distribution functions (and corresponding static structure factors) are considered.

Polar Tridimensional Network. All of the IL structures in Figure 5, from C_2mim to $C_{12}mim$, exhibit polar (red) domains that become more and more permeated by nonpolar (green) regions but, nevertheless, manage to preserve their continuity. An analogy can be made to a gel, where, despite the eventual swelling of the system, the interconnectivity of the cross-linked phase remains intact.

To confirm the persistence of the polar structure as the alkyl-chain length increases, we first analyzed the anion−anion center-of-mass RDFs, shown in Figure 6a. It is obvious that the anion−anion distances remain the same in all ILs, meaning that the presence of longer alkyl chains will have to be accommodated for without disruption of the cation−anion network and their characteristic distances.

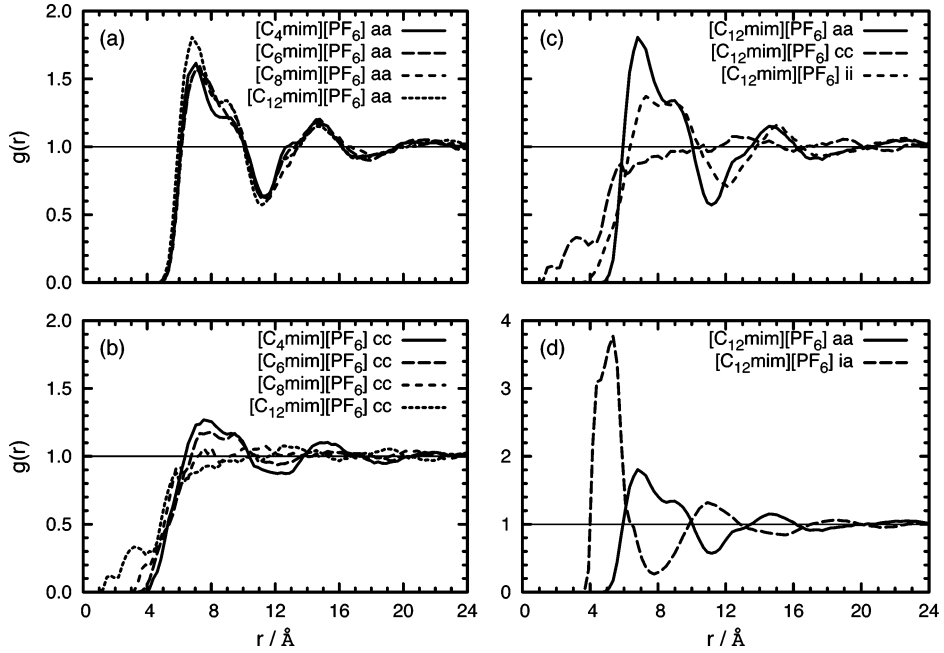

Figure 6. Center-of-mass radial distribution functions between anion−anion (aa) and cation−cation (cc) pairs in [$C_n$mim][PF_6]. Pairs denoted as ii and ia correspond to (the centers of mass of) the imidazolium rings in the cations relative to each other and relative to the anion, respectively.

The analysis of the cation−cation center-of-mass RDFs shown in Figure 6b does not yield such a clear picture: although the positions of the first peaks remain constant for C_4mim and C_6mim, the height and definition of these peaks diminish as the alkyl chain becomes longer. This is the consequence of two factors: First, in cations with longer side chains, a higher proportion of the atoms do not belong to the polar network. Second, the fact that the larger cations are more flexible in their conformations means that the center of mass is away from the polar headgroups and may even be positioned somewhere "outside" the molecule. Therefore, a RDF considering the center of mass of entire cations cannot capture correctly the structure of the polar domain.

Thus, we calculated for [C_{12}mim][PF_6] the cation−cation RDF considering only the centers of mass of the imidazolium rings and the adjacent atoms (the atoms colored red in Figure 4). The RDFs presented in Figure 6c are similar to those obtained for the anion−anion pairs and emphasize that only the imidazolium rings and the adjacent atoms belong to the polar network. Conclusions similar to the ones drawn for the anion−anion RDFs can be reached.

Finally, the RDF between the (center of mass of the) anion and the center of mass of the imidazolium ring (including adjacent atoms) was considered, and it is shown in Figure 6d. The most conspicuous feature of this RDF, when taken together with the anion−anion and cation−cation RDFs, is that the former function is in opposition of phase with the latter two, the typical charge-ordering structure being recovered. Such behavior is logical if we take into account the electrostatic nature of the interactions between anions and cations: the first neighbor shell of a given ion is always populated by ions with inverse charge (hetero interactions), the second shell, by ions with charges of the same sign (homo interactions), and so forth. This means that the homo pair RDFs (e.g., anion−anion) will have peaks and troughs corresponding to even and odd-shell distances, respectively, while the inverse is valid for the hetero pair RDFs (anion-imidazolium ring of cation).

The final demonstration of the persistence of the polar network from C_4mim to C_{12}mim is that this out-of-phase behavior is apparent in all ILs with the nodes appearing always at the same distance (cf. Figure 6a together with Figure 6d).

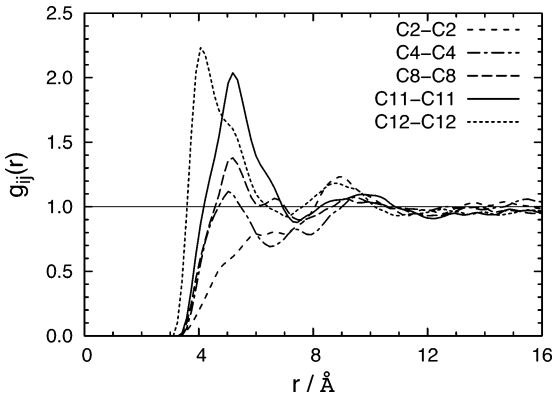

Figure 7. Intermolecular atom−atom radial distribution functions between several equivalent carbons along the alkyl side-chain in [C_{12}mim][PF_6].

Nonpolar Domains. The formation of a nonpolar domain was first suggested by analysis of the alkyl-chains' end carbon RDFs (see Figure 2 and the corresponding discussion). Here, we try to convey structural information about the typical size and topology of the nonpolar domains. RDFs taking into account all the atoms of the side-chain do not yield any insightful results since these RDFs do not show pronounced peaks, due to the multiple possible combinantions (and therefore distances) of pairs of atoms along the alkyl chain.

One solution is to select only some pairs of carbon atoms. Such a procedure was implemented for [C_{12}mim][PF_6], and Figure 7 represents the RDFs between pairs of equivalent carbon atoms as one moves along the alkyl chain, from its end carbon, C12, toward the imidazolium ring: C11, C8, C4, and C2. The trend is obvious: as we proceed along the chain toward the ring, the first peak decreases in intensity until we see a trough for C2. There is stronger spacial correlation between the ends of the tails than between the parts of the chain that are closer to the polar headgroup. This is an analogous situation to that found in spherical micelles.

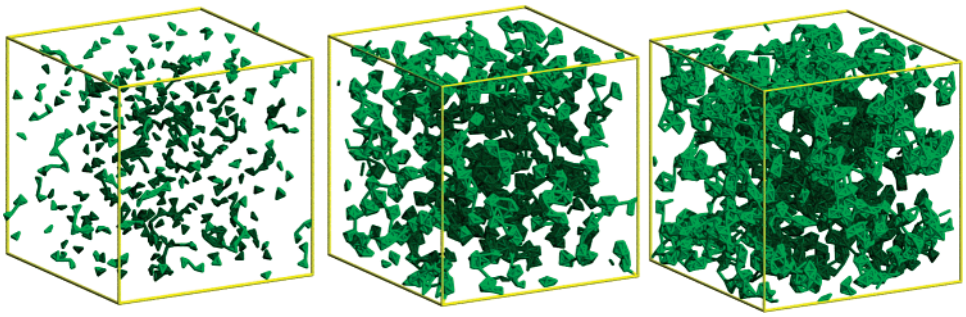

Figure 8. Topology of the nonpolar domains. The snapshots are of simulation boxes containing 700 ions of $[C_n\text{mim}][PF_6]$ with only the atoms of the nonpolar domain represented: (left) $[C_2\text{mim}][PF_6]$; (middle) $[C_4\text{mim}][PF_6]$; (right) $[C_6\text{mim}][PF_6]$.

The C4−C4 RDF in $[C_{12}\text{mim}][PF_6]$ (Figure 2) can be compared to the end-carbon RDF in $[C_4\text{mim}][PF_6]$ (Figure 7). Interestingly, for C4−C4, the first peak corresponds to a probability slightly higher than that found for the isotropic bulk density (1 in the normalized scale) whereas for the end-carbon of $[C_4\text{mim}][PF_6]$ the RDF shows a strong first peak, meaning that spacial correlation is stronger between the terminal carbons of the chains, even if they are of different lengths. It is observed that the nonpolar domains in the ILs become thicker as the alkyl chain lengthens, as illustrated in Figure 8. Connectivity between nonpolar regions is absent in $[C_2\text{mim}][PF_6]$, already present in $[C_4\text{mim}][PF_6]$, and ubiquitous in $[C_6\text{mim}][PF_6]$.

From Microdisperse to Bicontinuous Microphases. When the information gathered in the two previous sections is put together, i.e., one persistent tridimensional polar network becomes permeated with increasingly larger nonpolar domains, the evolution observed in the snapshots of Figure 5b−f can be understood. We are now in position to quantify the characteristic length scales of such structures. To achieve that, the radial distribution functions between centers of mass (COMs) belonging to the polar (red) and nonpolar (green) regions were calculated. The "red" COMs are those of the anions and of the imidazolium rings (and adjacent atoms) in the cations; the "green" COMs are those of the alkyl chains. The static partial structure factors, $S_{ij}(k)$, corresponding to the partial RDFs, $g_{ij}(r)$, were calculated by Fourier transform according to eq 1, where ρ is the number density of centers of mass considered (two in each cation and one in each anion).

$$S_{ij}(k) = 1 + \frac{4\pi\rho}{k}\int_0^\infty [g_{ij}(r) - 1] r \sin(rk)\, dr \qquad (1)$$

To obtain a total structure factor, the partial structure factors were combined using eq 2,[2] where x is a fraction of the centers of mass: $x_{red} = {}^2/_3$ and $x_{green} = {}^1/_3$.

$$S(k) = \sum_i \sum_j x_i x_j S_{ij}(k) \qquad (2)$$

The results for the total structure factors for a series of ILs are shown in Figure 9.

The most conspicuous features in the structure factors are the strong peaks around 1.4 $Å^{-1}$ that correspond to a wavelength of around $2\pi/1.4 = 4.5$ Å, i.e., to the distances between successive neighbor shells in the liquid structure (irrespective of the green or red nature of the neighbors) and a smaller peak around 0.2 $Å^{-1}$ corresponding to a wavelength of around 30 Å, which is the size of the simulation boxes and also the cutoff distance in the RDFs. No attempt was made to artificially extend the range of the radial distribution functions in order to correct the behavior of the structure factors at short reciprocal lengths and, in this manner, eliminate artificially such a peak. The region

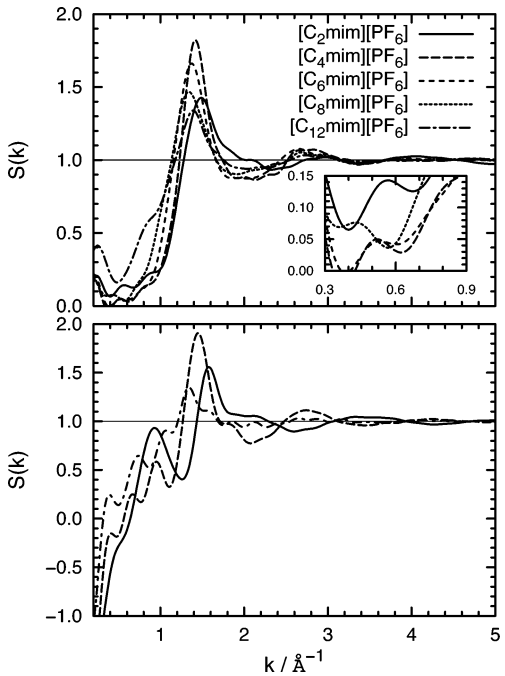

Figure 9. Static structure factors for $[C_n\text{mim}][PF_6]$ calculated from radial distribution functions: (top plot) total structure factor considering the centers of mass of the polar and nonpolar atom groups from the cation and the anion; (bottom plot) partial structure factors between centers of mass of the nonpolar regions.

TABLE 1: Length Scales of the Polar/Nonpolar Domains Obtained from Analysis of the Static Structure Factors, in Ionic Liquids with Increasing Alkyl-Chain Length

ionic liquid	peak wavenumber ($Å^{-1}$)	length scale (Å)
$[C_2\text{mim}][PF_6]$	0.56	11
$[C_4\text{mim}][PF_6]$	0.52	12
$[C_6\text{mim}][PF_6]$	0.50	13
$[C_8\text{mim}][PF_6]$	0.43	15
$[C_{12}\text{mim}][PF_6]$	0.3	20

of interest to evaluate the characteristic wavelength of the polar/nonpolar domains lies between those two peaks, namely, the small peaks at about 0.4−0.5 $Å^{-1}$ (see inset in Figure 9). The peak for $[C_{12}\text{mim}][PF_6]$ could not be accurately resolved due to its superposition with the peak of the box boundary, but its position could nevertheless be inferred approximately. The peak wavenumbers correspond to the length scales presented in Table 1. The domains' length scales in the different ionic liquids can be visualized by comparing the values in Table 1 with the pictures in Figure 5, taking into account the lengths of the simulation boxes given in the figure caption.

From the total structure factors (Figure 9 top plot), it would seem that the structure of $[C_2\text{mim}][PF_6]$ resembles closely that of the remaining ILs. However, a closer analysis of the partial

structure factor corresponding to the nonpolar regions only (Figure 9 bottom plot) shows, through the succession of peaks at short reciprocal lengths present in the long-chain ILs, that structuring of the nonpolar domains is indeed absent in $[C_2mim][PF_6]$. The peaks at short reciprocal lengths in the total structure factor of $[C_2mim][PF_6]$ are due to structuring of the polar domain.

Conclusion

Computer simulation using an all-atom force field predicted that pure ionic liquids of the 1-alkyl-3-methylimidazolium family show structuring of their liquid phases in a manner that is analogous to microphase separation between polar and nonpolar domains. It was observed that the polar domain has the structure of a tridimensional network of ionic channels, whereas the nonpolar domain is arranged as a dispersed microphase for ethylmethylimidazolium ILs and as a continuous one for longer side-chains, such as hexyl, octyl, or dodecyl. In our systems, the butyl side-chain marks the onset of the transition from one type of structure to the other.

The present results agree with other simulation work reported in the literature, namely, by Urahata and Ribeiro[24] and by Wang an Voth,[25] although different system sizes, depths of analysis, and details in the description of molecular interactions were used in these other reports.

Although no direct experimental evidence at the molecular level was found in the literature to corroborate these simulation results, they can help to explain a number of other observations, already discussed in the Introduction. For example, we can now attribute the behavior in viscosity, diffusion coefficient, and ionic conductivity reported by Watanabe et al.[17] to the existence of those microdomains. Especially, the break in the trends of these properties observed between alkylmethylimidazolium ILs with C_n with $n = 1$ or 2 from those having $n = 4$, 6, or 8 coincides with the present results on the formation of the nanostructures.

We hope the present study will stimulate new experimental work to eventually validate the conclusions herein. The realization that pure room-temperature ionic liquids can be understood as nanostructured fluids, if verified, can lead to new insights on the many unique properties of these materials.

Acknowledgment. The authors acknowledge support under a collaboration program (PICS 3090) beween the Chemistry Department of CNRS, France, and the GRICES Office, Portugal.

References and Notes

(1) Rogers, R. D.; Seddon, K. R., Eds. *Ionic Liquids IIIA: Fundamentals, Progress, Challenges, and Opportunities — Properties and Structure*; ACS Symposium Series 901; American Chemical Society, Washington, D.C., 2005.

(2) Hansen, J. P.; McDonald, I. R. *Theory of Simple Liquids*, 2nd ed.; Academic Press: London, 1986.

(3) Hansen, J. P.; McDonald, I. R. *Phys. Rev. A* **1975**, *11*, 2111.

(4) Gordon, C. M.; Holbrey, J. D.; Kennedy, A. R.; Seddon, K. R. *J. Mater. Chem.* **1998**, *8*, 2627.

(5) Scröder, U.; Wadhawan, J. D.; Compton, R. G.; Marken, F.; Suarez, P. A. Z.; Consorti, C. S.; de Souza, R. F.; Dupont, J. *New J. Chem.* **2000**, *24*, 1009.

(6) Dupont, J. *J. Braz. Chem. Soc.* **2004**, *15*, 341.

(7) Consorti, C. S.; Suarez, P. A. Z.; de Souza, R. F.; Burrow, R. A.; Farrar, D. H.; Lough, A. J.; Loh, W.; da Silva, L. H. M.; Dupont, J. *J. Phys. Chem. B* **2005**, *109*, 4341.

(8) http://www.ccdc.cam.ac.ok/ (accessed Jan 2006).

(9) Hardacre, C.; Holbrey, J. D.; McMath, S. E. J.; Bowron, D. T.; Soper, A. K. *J. Chem. Phys.* **2003**, *118*, 273.

(10) Dieter, K. M.; Dymek, C. J., Jr.; Heimer, N. E.; Rovang, J. W.; Wilkes, J. S. *J. Am. Chem. Soc.* **1988**, *110*, 2722.

(11) Hayashi, S.; Ozawa, R.; o Hamagushi, H. *Chem. Lett.* **2003**, *32*, 498.

(12) Ozawa, R.; Hayashi, S.; Saha, S.; Kobayashi, A.; o Hamaguchi, H. *Chem. Lett.* **2003**, *32*, 948.

(13) Fannin, A. A., Jr.; King, L. A.; Levisky, J. A.; Wilkes, J. S. *J. Phys. Chem.* **1984**, *88*, 2609.

(14) Abdul-Sada, A. K.; Elaiwi, A. E.; Greenaway, A. M.; Seddon, K. R. *Eur. J. Mass Spectrom.* **1997**, *3*, 245.

(15) Gozzo, F. C.; Santos, L. S.; Augusti, R.; Consorti, C. S.; Dupont, J.; Eberlin, M. N. *Chem.—Eur. J.* **2004**, *10*, 6187.

(16) Anderson, J. L.; Armstrong, D. W. *Anal. Chem.* **2003**, *75*, 4851.

(17) Tokuda, H.; Hayamizu, K.; Ishii, K.; Susan, M. A. B. H.; Watanabe, M. *J. Phys. Chem. B* **2005**, *109*, 6103.

(18) Bonhôte, P.; Dias, A.-P.; Papageorgiou, N.; Kalyanasundaram, K.; Grätzel, M. *Inorg. Chem.* **1996**, *35*, 1168.

(19) Hanke, C. G.; Price, S. L.; Lynden-Bell, R. M. *Mol. Phys.* **2001**, *99*, 801.

(20) de Andrade, J.; Boes, E. S.; Stassen, H. *J. Phys. Chem. B* **2002**, *106*, 3546.

(21) Margulis, C. J.; Stern, H. A.; Berne, B. J. *J. Phys. Chem. B* **2002**, *106*, 12017.

(22) Morrow, T. I.; Maginn, E. J. *J. Phys. Chem. B* **2002**, *106*, 12807.

(23) del Pópolo, M. G.; Voth, G. A. *J. Phys. Chem. B* **2004**, *108*, 1704.

(24) Urahata, S. M.; Ribeiro, M. C. C. *J. Chem. Phys.* **2004**, *120*, 1855.

(25) Wang, Y.; Voth, G. A. *J. Am. Chem. Soc.* **2005**, *127*, 12192.

(26) Canongia Lopes, J. N. A. *Phys. Chem. Chem. Phys.* **2002**, *6*, 949.

(27) Canongia Lopes, J. N.; Deschamps, J.; Pádua, A. A. H. *J. Phys. Chem. B* **2004**, *108*, 2038.

(28) Canongia Lopes, J. N.; Pádua, A. A. H. *J. Phys. Chem. B* **2004**, *108*, 16893.

(29) Cornell, W. D.; Cieplak, P.; Bayly, C. I.; Gould, I. R.; Merz, K. M.; Fergusin, D. M.; Spellmeyer, D. C.; Fox, T.; Caldwell, J. W.; Kollman, P. A. *J. Am. Chem. Soc.* **1995**, *117*, 5179.

(30) Jorgensen, W. L.; Maxwell, D. S.; Tirado-Rives, J. *J. Am. Chem. Soc.* **1996**, *118*, 11225.

(31) Smith, W.; Forester, T. R., *The DL_POLY package of molecular simulation routines*, version 2.13; The Council for the Central Laboratory of Research Councils, Daresbury Laboratory: Warrington, UK, 1999.

(32) Yan, T.; Burnham, C. J.; del Pópolo, M. G.; Voth, G. A. *J. Phys. Chem. B* **2004**, *108*, 11877.